

# HSulf-1 and HSulf-2 Are Potent Inhibitors of Myeloma Tumor Growth *in Vivo*\*

Received for publication, July 25, 2005, and in revised form, September 15, 2005 Published, JBC Papers in Press, September 27, 2005, DOI 10.1074/jbc.M508136200

Yuemeng Dai<sup>‡</sup>, Yang Yang<sup>‡</sup>, Veronica MacLeod<sup>‡</sup>, Xinping Yue<sup>§</sup>, Alan C. Rapraeger<sup>§</sup>, Zachary Shriver<sup>¶</sup>, Ganesh Venkataraman<sup>¶</sup>, Ram Sasisekharan<sup>||</sup>, and Ralph D. Sanderson<sup>‡1</sup>

From the <sup>‡</sup>Department of Pathology and the Arkansas Cancer Research Center, University of Arkansas for Medical Sciences, Little Rock, Arkansas 72205, the <sup>§</sup>Department of Pathology and Laboratory Medicine, University of Wisconsin, Madison, Wisconsin 53706, <sup>¶</sup>Momenta Pharmaceuticals, Inc., Cambridge, Massachusetts 02142, and the <sup>||</sup>Biological Engineering Division, Massachusetts Institute of Technology, Cambridge, Massachusetts 02139

To participate as co-receptor in growth factor signaling, heparan sulfate must have specific structural features. Recent studies show that when the levels of 6-*O*-sulfation of heparan sulfate are diminished by the activity of extracellular heparan sulfate 6-*O*-endosulfatases (Sulfs), fibroblast growth factor 2-, heparin binding epidermal growth factor-, and hepatocyte growth factor-mediated signaling are attenuated. This represents a novel mechanism for regulating cell growth, particularly within the tumor microenvironment where the Sulfs are known to be misregulated. To directly test the role of Sulfs in tumor growth control *in vivo*, a human myeloma cell line was transfected with cDNAs encoding either of the two known human endosulfatases, HSulf-1 or HSulf-2. When implanted into severe combined immunodeficient (SCID) mice, the growth of these tumors was dramatically reduced on the order of 5- to 10-fold as compared with controls. In addition to an inhibition of tumor growth, these studies revealed the following. (i) HSulf-1 and HSulf-2 have similar functions *in vivo*. (ii) The extracellular activity of Sulfs is restricted to the local tumor cell surface. (iii) The Sulfs promote a marked increase in extracellular matrix deposition within tumors that may, along with attenuated growth factor signaling, contribute to the reduction in tumor growth. These findings demonstrate that dynamic regulation of heparan sulfate structure by Sulfs present within the tumor microenvironment can have a dramatic impact on the growth and progression of malignant cells *in vivo*.

Heparan sulfate proteoglycans act as co-receptors for numerous heparin-binding growth factors and cytokines and are thus key regulators of cell signaling (1). Previous studies have demonstrated that growth factor binding to heparan sulfate and the resulting mitogenic activity occur only when specific structural features are present within the heparan sulfate chains. These features include sulfation at specific positions within a disaccharide (*N*, 2-*O*, 3-*O*, 6-*O*) by the enzymes that orchestrate heparan sulfate synthesis within the Golgi (2). However, recent studies show that following its synthesis and expression, heparan sulfate can also be structurally and functionally modified within the extracellular compartment. The two enzymes presently known to have these effects are heparanase, which cleaves heparan sulfate chains into small, biologically active fragments, and the heparan sulfate 6-*O*-endosulfatases

(Sulfs).<sup>2</sup> Sulfs represent a newly discovered family of enzymes that are secreted via the Golgi and become localized to the cell surface or are released into the extracellular matrix. These enzymes selectively remove the 6-*O*-sulfate groups from heparan sulfate with preference for the 6-*O*-sulfates present on trisulfated disaccharides (3, 4).

The first member of the endosulfatase family to be described was sulfatase-1 from quail (QSulf1), where the activity of this enzyme is required for Wnt-mediated signaling in developing muscle (5). In separate studies, QSulf1 was shown to restore bone morphogenetic protein signaling in cells by releasing its functional inhibitor, Noggin, from cell surfaces (3). In contrast, QSulf1 can also inhibit growth factor signaling, as removal of the 6-*O*-sulfation required for the formation of the FGF·HS·FR1c ternary complex blocks FGF2 signaling (6). Thus, the Sulfs can have activities that promote or inhibit growth factor signaling depending on the specific factor involved.

In addition to quail, the Sulf-1 enzyme has also been cloned from rat, mouse, and human, and a second family member, Sulf-2, has been cloned from both mouse and humans (7, 8). Sulf-2 is very similar in structural organization to Sulf-1 but is somewhat divergent in sequence identity (64%) in humans. Both Sulf-1 and Sulf-2 show high specificity for 6-*O*-sulfates of the trisulfated disaccharides of heparin at neutral pH (7).

Analysis of human tumor tissue and tumor cell lines suggests that HSulf-1 is misregulated in cancer. HSulf-1 is present in a variety of normal tissues but is down-regulated in tumor cell lines originating from ovarian, breast, pancreatic, renal, and hepatocellular carcinoma (9). Re-expression of HSulf-1 in an ovarian cell line diminishes FGF-2 and heparin-binding epidermal growth factor (HB-EGF) signaling and cell proliferation *in vitro* and enhances drug-induced apoptosis (9). Further evidence of the role of HSulf-1 as a negative regulator of tumor cell growth was also found in cell lines derived from squamous cell carcinoma of the head and neck. In these cells, expression of HSulf-1 inhibits growth as well as HGF signaling, resulting in inhibition of tumor cell motility and invasion *in vitro* (10). In tumor tissues harvested from cancer patients, HSulf-1 is sometimes elevated and sometimes diminished as compared with normal tissue, leaving open the question of the role of this enzyme in tumorigenesis and progression *in vivo* (9, 11, 12).

To directly assess the effect of Sulf expression on tumor growth *in vivo*, we implanted human myeloma cells transfected with the cDNA for either HSulf-1 or HSulf-2 into SCID mice. Expression of Sulfs has no

\* This work was supported by National Institutes of Health Grants CA68494 and CA55819 (to R. D. S.). The costs of publication of this article were defrayed in part by the payment of page charges. This article must therefore be hereby marked "advertisement" in accordance with 18 U.S.C. Section 1734 solely to indicate this fact.

<sup>1</sup> To whom correspondence should be addressed: Dept. of Pathology, University of Arkansas for Medical Sciences, 4301 West Markham St., Little Rock, AR 72205. Tel.: 501-686-6413; Fax: 501-686-5168; E-mail: RDSanderson@uams.edu.

<sup>2</sup> The abbreviations used are: Sulf, heparan sulfate 6-*O*-endosulfatase; AP, alkaline phosphatase; ECM, extracellular matrix; EGFP, enhanced green fluorescent protein; ERK, extracellular signal-regulated kinase; FGF, fibroblast growth factor; FR1c, fibroblast growth factor receptor 1c; HGF, hepatocyte growth factor; HS, heparan sulfate; HSulf, human Sulf; PBS, phosphate buffered saline; QSulf, quail Sulf; SCID, severe combined immunodeficient (mice).

effect on tumor cell growth *in vitro*, but *in vivo* we find that enhanced Sulf expression dramatically and consistently inhibits growth of these tumors. Tumors formed by cells expressing Sulf exhibit evidence of enhanced extracellular matrix deposition, yet they are unable to assemble the FGF-2 ternary signaling complex on the tumor cell surface. We conclude that 6-*O*-sulfation of heparan sulfate by myeloma tumor cells is a critical determining factor regulating the *in vivo* growth of this cancer.

## EXPERIMENTAL PROCEDURES

**Cells and Transfections**—CAG cells were established from a bone marrow aspirate of a myeloma patient at our center as described previously (13). This cell line secretes human  $\kappa$  light chain, is Epstein-Barr virus negative, and will form tumors when injected subcutaneously in SCID mice (14). Cells were cultured in RPMI 1640 medium supplemented with 10% fetal bovine serum, 2 mM L-glutamine, 100 units/ml penicillin, and 100  $\mu$ g/ml streptomycin sulfate.

The pcDNA3.1/myc-His(-) vector containing the coding region of HSulf-1 or HSulf-2, respectively, were kindly provided by Dr. Steven D. Rosen (University of California, San Francisco, CA) (7). To insert the HSulf-1 or HSulf-2 coding region into the expression plasmid pIRES2-EGFP (Clontech), the full-length DNA fragments were amplified by PCR of pcDNA3.1/myc-His(-) vectors. The forward and reverse primers were 5'-GCCCTCTAGACTCGAGACAATGAAGTA-3' (forward) and 5'-CGGTTAACCTTCCATCCATCCCATA-3' (reverse) for HSulf-1 and 5'-GTTTAAACGGGCCCTCTAGACTCG-3' (forward) and 5'-TCTAGAAATTAACCTTCCAGCCTTCC-3' (reverse) for HSulf-2. The XhoI restriction site shown in boldface type was introduced into the forward primers, and the stop codons of HSulf-1 and HSulf-2 were restored in the reverse primers. The Expand long template PCR System (Roche Applied Science) was applied in the PCR procedure. Briefly, after initial denaturation, PCR was carried out for the first 10 cycles (94 °C for 10 s; 55 °C for 30 s; and 68 °C for 2 min per cycle) and then for another 25 cycles (94 °C for 15 s; 55 °C for 30 s; and 68 °C for 2 min + 5 s per cycle). PCR products were purified from 1% low melting temperature agarose gels (BioWhittaker Molecular Applications, Rockland, ME) using a gel extraction kit (Qiagen, Valencia, CA) and subcloned into the pGEM-T vector (Promega, Madison, WI) with T4 DNA ligase (Promega). The constructs were confirmed by sequencing and then digested with XhoI and SalI. The digested HSulf-1 and HSulf-2 cDNAs were again purified from 1% low melting temperature agarose and then subcloned into the corresponding sites of pIRES2-EGFP, and the inserts were confirmed by sequencing.

The pIRES2-EGFP/HSulf-1 or pIRES2-EGFP/HSulf-2 construct (10  $\mu$ g of DNA) or, as a control, the pIRES2-EGFP vector containing no insert was transfected into the CAG cells using Lipofectamine 2000 (Invitrogen) and Opti-MEM I (Invitrogen) per the manufacturer's instructions. Once cell numbers reached  $2.0 \times 10^7$ , both the sulfatase transfectants and control transfectants were sorted by flow cytometry using EGFP expression. Over time, at least three sortings were performed to enhance the population of fluorescent cells. All experiments were performed using populations of cells that had a minimum of 70% cells expressing EGFP.

**Analysis of Heparan Sulfate Disaccharide Composition**—Cells ( $1 \times 10^7$ ) were harvested and then treated with 70  $\mu$ g of bacterial heparinase III in 2.5 ml of phosphate-buffered saline (PBS) at 37 °C on a shaker for 1 h. After centrifugation at 2000 rpm for 5 min, the supernatants were collected, boiled for 15 min, and filtered through a 0.22- $\mu$ m filter. The heparan sulfate fragments in the supernatants released by heparinase III digestion were digested overnight at 37 °C with proteinase K. After

digestion, residual fragments were extracted via the addition of 1 volume of phenol/chloroform. The aqueous layer containing the heparan sulfate fragments was dried via Speed Vac and resuspended in water. Further digestion of heparan sulfate to disaccharides was accomplished using a mixture of heparinases I–III obtained via recombinant expression of the enzymes in *Escherichia coli*. Four hundred milliunits of each enzyme were added to the aqueous heparan sulfate material and incubated overnight at 30 °C. The material was analyzed by capillary electrophoresis using a high sensitivity flow cell in reverse polarity under conditions of electrophoretic flow with minimal electroosmotic flow (15).

**Immunostaining for Heparan Sulfate**—For immunohistochemistry, antigen retrieval on slides was performed using citrate buffer solution (pH 6.0) (Zymed Laboratories Inc.) in a steamer for 20 min followed by blocking of endogenous peroxidase with 3% hydrogen peroxide for 10 min. After blocking for 30 min with PBS containing 5% nonfat dry milk, sections were incubated with monoclonal antibody 10E4 (Seikagaku America, Falmouth, MA) (16) followed by biotin-conjugated anti-mouse IgM (Vector Laboratories, Inc., Burlingame, CA). Vector ABC solution was added to enhance sensitivity of detection. Peroxidase staining was visualized with a 3,3'-diaminobenzidine solution (Vector Laboratories, Inc.) until the desired stain intensity developed, and the sections were lightly counterstained in Mayer's hematoxylin. Because 3% hydrogen peroxide can degrade heparan sulfates, as a control the tissues were also stained without the 3% hydrogen peroxide blocking step. Removal of the 3% hydrogen peroxide blocking step resulted in overall higher background staining but had no effect on the detection of relative levels of 10E4 staining as compared between control-transfected and HSulf-transfected cells (data not shown).

For flow cytometry, cells ( $1.0 \times 10^6$ ) were harvested from culture, washed twice with PBS, and incubated for 45 min on ice with a 1:50 dilution of mouse 10E4 antibody. After washing, cells were stained with 1:100 dilution of phycoerythrin-conjugated anti-mouse IgM for 30 min on ice. Cells were washed three times in PBS and analyzed by flow cytometry (FACScan; BD Biosciences).

**Protein Isolation and Western Blotting**—Cells in culture ( $3 \times 10^6$ ) were pelleted by centrifugation, rinsed with ice-cold PBS, and lysed on ice in T-PER<sup>TM</sup> tissue protein extraction reagent (Pierce) with the protease inhibitors *N*-ethylmaleimide (5 mM), benzamide (5 mM), and phenylmethylsulfonyl fluoride (1 mM). Lysates were centrifuged at 13,000 rpm for 10 min at 4 °C, and supernatants were frozen at -80 °C. Prior to Western blotting, protein concentrations of lysates were determined using a BCA protein assay reagent kit (Pierce). Equal amounts of protein were loaded onto 4–12% SDS-polyacrylamide gels for electrophoresis, transferred to a nitrocellulose membrane, and probed with polyclonal antibodies against Sulf-1 or Sulf-2 (kindly provided by Dr. Charles P. Emerson, Jr., Boston Biomedical Institute, Boston, MA). Following incubation with a horseradish peroxidase-conjugated donkey anti-rabbit IgG (Amersham Biosciences), immunoreactive bands were detected using chemiluminescence (Amersham Biosciences).

**Analysis of Tumor Growth *in Vivo***—For establishing subcutaneous tumors, control-transfected or Sulf-transfected cells ( $1.0 \times 10^6$ ) were suspended in 100  $\mu$ l of PBS and injected subcutaneously into the left flanks of SCID mice. Tumor growth was monitored by visual inspection and by determination of  $\kappa$  light chain levels present in murine serum by enzyme-linked immunosorbent assay as described previously (17). All samples were analyzed in duplicate simultaneously to preclude interassay variability. The standard curve was linear between 0.35 and 300 ng/ml, and samples were diluted to concentrations within this range. Seven weeks after the injection of tumor cells, the animals were eutha-

## Extracellular Sulfatase Inhibits Tumor Growth *in Vivo*

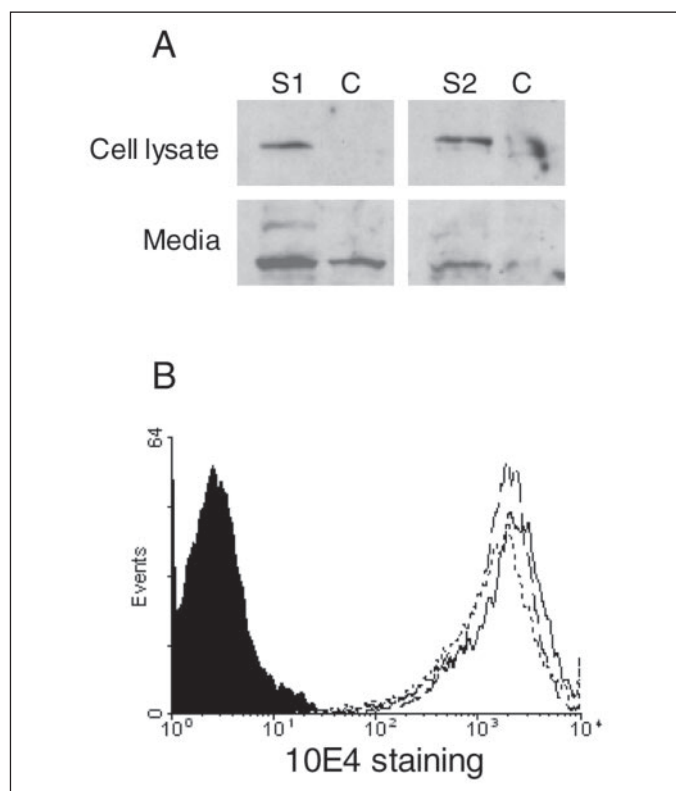


**FIGURE 1. Elevated levels of HSulf-1 and HSulf-2 are present in transfected CAG cells.** A, HSulf-1-transfected (S1) or HSulf-2-transfected (S2) cells express the enzyme in cell lysates and in conditioned media. Western blots were probed with a polyclonal antibody that recognizes both Sulfs migrating at ~130 kDa. Note that low levels of endogenous Sulfs are present in the conditioned media from control cells transfected with empty vector (C). B, expression of HSulf-1 or HSulf-2 does not alter levels of staining with antibody 10E4. Control-transfected (solid line), HSulf-1-transfected (dashed line), and HSulf-2-transfected (dotted line) CAG cells all stain brightly positive with antibody 10E4. Control-transfected cells stained with second antibody only are negative (shaded peak).

nized, the primary tumor was excised, and the wet weight was determined. Tumor tissue was then divided, and a portion was immediately frozen at  $-80^{\circ}\text{C}$ . The remaining portion of tumor tissue was fixed in 10% formalin, pH 7.0, and embedded in paraffin. Tissue sections were stained with hematoxylin and eosin for routine histological examination or with Masson's trichrome stain for visualization of collagen.

**Analysis of FGF-2 Signaling**—Determination of the ERK expression level was used as a reflection of FGF-2 mediated signaling *in vitro*. Cells ( $3.0 \times 10^6$ ) were serum starved for 12–15 h and treated with 2 ng/ml FGF-2 (R&D Systems, Minneapolis, MN) for 1 h at  $37^{\circ}\text{C}$ . Following treatment, cells were rinsed with ice-cold PBS and lysed on ice in T-PER<sup>TM</sup> tissue protein extraction reagent (Pierce) with protease inhibitors as described above. Protein concentrations were determined by BCA assay (Pierce). Equal amounts of protein (80  $\mu\text{g}/\text{lane}$ ) were separated by electrophoresis on 4–12% Tris-glycine SDS-polyacrylamide gels (Invitrogen) and electrotransferred onto a nitrocellulose membrane. Blots were washed once with Tris-buffered saline and 0.1% Tween 20 (TBST) and blocked with TBST containing 5% nonfat dry milk for 30 min at room temperature. The blocking solution was replaced with a fresh solution containing 1:1000 dilution of rabbit anti-phospho-ERK (Cell Signaling Inc., Beverly, MA). After overnight incubation at  $4^{\circ}\text{C}$ , the blot was washed three times for 10 min each in TBST and incubated with 1:2500 dilution of horseradish peroxidase-conjugated secondary antibody in TBST at room temperature for 1 h. After washing four times in TBST, the proteins were visualized using

enhanced chemiluminescence (Amersham Biosciences). The blots were stripped with Restore<sup>TM</sup> Western blot stripping buffer (Pierce) for 15 min at room temperature and reprobed with 1:1000 dilution of rabbit anti-total-ERK (Cell Signaling Inc.) at  $4^{\circ}\text{C}$ , overnight, followed by incubation with 1:2500 dilution of horseradish peroxidase-conjugated secondary antibody in TBST at room temperature for 1 h. After washing four times in TBST, the proteins were visualized using enhanced chemiluminescence, and the bands were quantified using ImageJ 1.33u software (National Institutes of Health).

**Analysis of FGF-2 Binding and FGF-2-HS-FR1cAP Formation**—For analysis of the assembly of the FGF-2-HS-FR1c signaling complex *in situ*, frozen sections (5  $\mu\text{m}$ ) of primary tumors were air-dried and fixed for 10 min in 4% paraformaldehyde on ice. Sections were then incubated in PBS at  $65^{\circ}\text{C}$  for 20 min to inactivate endogenous alkaline phosphatase (AP). Prior to the binding assays, sections were incubated with PBS containing 2 M NaCl to remove any endogenous FGFs that may have been bound to the heparan sulfate on the tissue sections. Samples were then blocked in binding buffer (PBS containing 1 mM  $\text{Ca}^{2+}$ , 0.5 mM  $\text{Mg}^{2+}$ , and 0.5% bovine serum albumin) for 1 h before the binding assays. First, to determine whether heparan sulfate levels were the same in tumors formed from control- and Sulf-transfected cells, total heparan sulfate distribution was estimated using the monoclonal antibody 3G10 (Seikagaku America, Falmouth, MA), which recognizes the unsaturated uronic acid residue of heparan sulfate remaining on the core protein following heparin lyase digestion (16). For this purpose, sections were incubated with 10 milliunits/ml heparinase I and III (IBEX Technologies Inc., Montreal, Quebec, Canada) in the binding buffer for 2 h at  $37^{\circ}\text{C}$  before 3G10 detection (1:200) using the mouse on mouse (M. O. M.<sup>TM</sup>) immunodetection kit from Vector Laboratories, Inc. This was followed by incubation with AP-conjugated donkey anti-mouse secondary antibody and nitro blue tetrazolium/5-bromo-4-chloro-3-indolyl phosphate substrate (Roche Applied Science) detection of alkaline phosphatase. Sections without prior heparinase treatment were used as the antibody control.

To examine FGF-2 binding to tumor heparan sulfate, sections were incubated with 5 nM FGF-2 (Peprotech, Rocky Hill, NJ) in binding buffer for 1 h at room temperature. For FGF-2-FR1c complex formation, 5 nM FGF-2 and 5 nM FR1cAP (see below) were added to the binding buffer together and applied to the sections for 1 h at room temperature. FR1cAP is a soluble FGF receptor 1c fusion protein that consists of the three extracellular Ig loop domains of the IIIc splice variant of FR1c fused to the  $\text{NH}_2$  terminus of human placental alkaline phosphatase (18). The FR1cAP fusion protein was purified as described previously (19) and quantified based on its AP activity (20, 21). Following incubation with FGF-2 or FGF-2 and FR1cAP, sections were washed three times in PBS containing  $\text{Ca}^{2+}$  and  $\text{Mg}^{2+}$ . Bound FGF-2 was detected with DE6 anti-FGF-2 antibody (1:200, a gift of Dupont) followed by an AP-conjugated donkey anti-mouse secondary antibody. For detection of FGF-2-HS-FR1cAP complexes, sections were incubated directly with the AP substrate nitro blue tetrazolium/5-bromo-4-chloro-3-indolyl phosphate, which forms purple precipitates at the sites of AP activity. To confirm that the above binding assays were heparan sulfate-dependent, one set of sections was treated with heparinases I and III as described for 3G10 staining before the addition of FGF-2 or FGF-2-FR1cAP.

## RESULTS

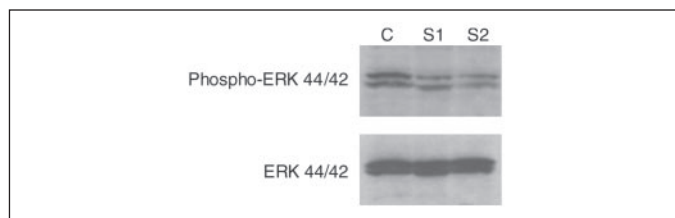
**HSulf-1 and HSulf-2 Remove 6-O-Sulfates from the Surface of Myeloma Cells and Attenuate FGF-2 Signaling *in Vitro***—CAG myeloma cells were transfected with vector containing the cDNA for

TABLE ONE

**Expression of Sulfs diminishes 6-O-sulfation of trisulfated disaccharides**

Heparan sulfate was removed from the surface of cells by treatment with bacterial heparinase III and analysed for disaccharide composition by capillary electrophoresis. Results are expressed as the percentage of area within individual peaks of the electrophoretic profile. C, control cells; S1, HSulf-1-transfected cells; S2, HSulf-2-transfected cells.

	$\Delta U_{25H_{NS,6S}}$	$\Delta U_{25H_{NS}}$	$\Delta UH_{NS,6S}$	$\Delta UH_{NS}$	$\Delta UH_{NAC,6S}$	$\Delta UH_{NAC}$
C	10	12	14	19	5	40
S1	3	19	12	21	3	41
S2	5	21	10	17	7	39



**FIGURE 2. Enhanced expression of HSulf-1 or HSulf-2 diminishes FGF-2 downstream signaling.** Control-transfected (C), HSulf-1-transfected (S1), or HSulf-2-transfected (S2) cells were serum-starved for 12 h, exposed to exogenous FGF-2, and extracted. Cell lysates were electrophoresed, transferred to nitrocellulose, and probed with antibodies to detect either phosphorylated or total ERK.

either HSulf-1 or HSulf-2. Following multiple rounds of selection, cell extracts and conditioned media from cultured cells were analyzed by Western blotting. Results show that both cells and media from HSulf-1 and HSulf-2 transfectants exhibit enhanced levels of enzyme as compared with controls transfected with empty vector alone (Fig. 1A). To determine whether Sulf expression alters heparan sulfate structure on the cell surface, the cells were stained with 10E4, an antibody specific for heparan sulfate chains (16). Previous studies have shown that expression of Sulfs reduces the amount of 10E4 epitope detectable on the cell surface (4, 9). However, staining of the Sulf-transfected myeloma cells with antibody 10E4 indicated no difference in the level of staining between controls and cells expressing elevated levels of Sulfs (Fig. 1B). This result raised concern that the Sulfs may not be enzymatically active when expressed in myeloma cells.

To directly test whether the Sulfs were active, the transfected cells were treated with bacterial heparinase III, and the released heparan sulfate fragments were analyzed for their disaccharide composition. As compared with control cells, the cells expressing either HSulf-1 or HSulf-2 exhibit a significant reduction (70 and 50%, respectively) in 6-O-sulfates present in  $\Delta U_{25H_{NS,6S}}$  trisulfated disaccharides with a concomitant increase in the amount of the disulfated disaccharide  $\Delta U_{25H_{NS}}$  (TABLE ONE). The overall levels of 6-O monosulfated ( $\Delta UH_{NAC,6S}$ ) and 6-O disulfated disaccharides ( $\Delta UH_{NS,6S}$ ) show generally smaller reductions in their levels as compared with controls. These findings point to a general specificity of the HSulfs for the highly bioactive trisulfated disaccharides as has been described previously (3, 4).

To determine whether reduction in 6-O-sulfation on these cells has a biological effect, we examined FGF-2 signaling. Previous studies have demonstrated that HSulf-1 and Qsulf-1 expression can suppress FGF-2 signaling, presumably by removing 6-O-sulfates critical for the promotion of signaling via FGF receptors (6, 9, 22–24). CAG control and Sulf-transfected cells were serum-starved for 12 h and stimulated with FGF-2, and downstream signaling was analyzed by determining the levels of phosphorylated ERK 44/42 (ERK1 and ERK2). Western blots of cell extracts reveal that cells transfected with either HSulf-1 or HSulf-2 exhibit diminished levels of phosphorylated ERK as compared with control (Fig. 2). This finding, coupled with the biochemical data (TABLE ONE), confirms that both Sulfs are enzymatically active in removing

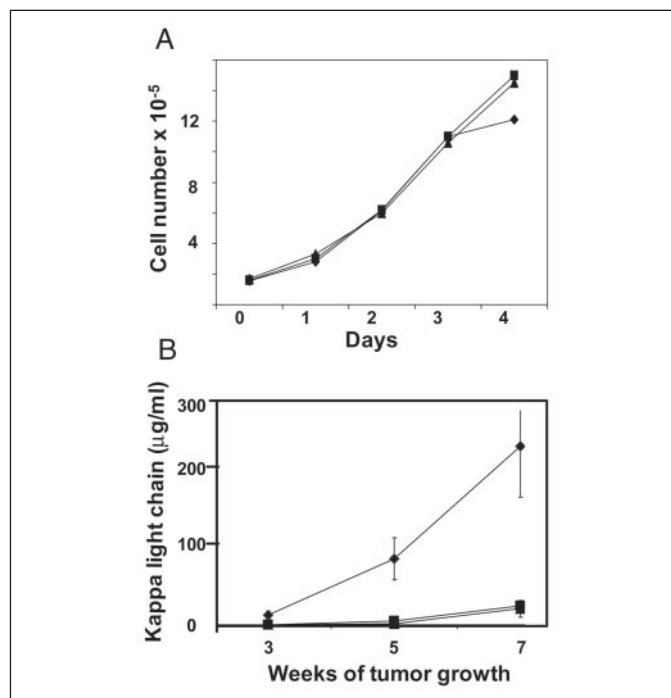


**FIGURE 3. Enhanced expression of HSulf-1 or HSulf-2 inhibits tumor cell growth *in vivo* but not *in vitro*.** A, control-transfected ( $\blacklozenge$ ), HSulf-1-transfected ( $\blacksquare$ ), or HSulf-2-transfected ( $\blacktriangle$ ) cells were plated in equal numbers in cell culture flasks and counted on four consecutive days. B, cells were injected subcutaneously at a single site in SCID mice, and whole animal tumor burden was assessed by determination of human  $\kappa$  light chain levels in the sera harvested from animals. ( $p < 0.0004$  for control versus either HSulf-1 or HSulf-2 at 7 weeks;  $n = 6$  animals/group.)

6-O-sulfates of trisulfated disaccharides and that expression of either of these enzymes diminishes the cell signaling events that control growth and other cell behaviors.

**Expression of Sulfs Inhibits Tumor Growth *in Vivo***—Comparison of control and Sulf-transfected cells growing in serum-containing media shows that the cells proliferate at approximately the same rate *in vitro* (Fig. 3A). To test the effect of Sulf expression *in vivo*, tumor cells were injected subcutaneously into SCID mice, and serum levels of the human  $\kappa$  light chain were monitored as an indicator of whole animal tumor burden (17). Results indicate that expression of either HSulf-1 or HSulf-2 dramatically inhibits *in vivo* growth of the tumors as compared with control-transfected cells (Fig. 3B). Two subsequent experiments showed the same level of inhibition in tumors formed by the Sulfs. Data in Fig. 4 are expressed as a plot of the weight of each primary tumor harvested in the three consecutive experiments (overall mean tumor weights are 2.44, 0.46, and 0.18 g for controls, HSulf-1, and HSulf-2, respectively). For visual comparison, Fig. 5A shows the primary tumors harvested from the second experiment.

**Sulf Expression Enhances ECM Deposition within Tumor Stroma**—When sections of tumors were stained with the antibody 10E4 to assess heparan sulfate expression, very little staining was detected on the sur-

## Extracellular Sulfatase Inhibits Tumor Growth *in Vivo*

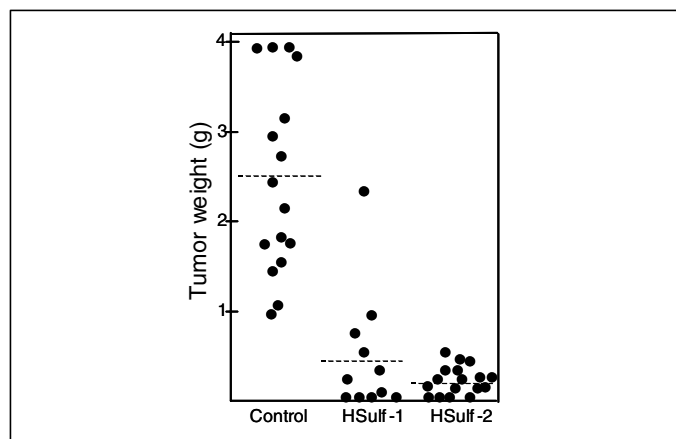


FIGURE 4. **HSulf-1 and HSulf-2 inhibit tumor growth *in vivo*.** The weight of primary tumors was plotted for each of the three groups of animals. Each dot represents the primary tumor weight from a single animal injected at a single site. The data are cumulative of three separate experiments. Dots lying on the x-axis represent animals in which visible tumors could not be detected at necropsy. The dashed lines represent the mean tumor weight for each group. ( $p < 0.0001$  for control versus either HSulf-1 or HSulf-2.)

face of any of the tumor cells (Fig. 5B, top). This observation is in contrast to the *in vitro* results showing bright 10E4 staining on all the cells (Fig. 1B). The lack of cell surface staining *in vivo* is likely due to epitope masking (see "Discussion"). However, 10E4 staining does reveal a striking elevation in the amount of heparan sulfate present within the stromal ECM of Sulf-expressing tumors as compared with controls (Fig. 5B, top row). This finding suggests that the deposition of ECM may be enhanced by expression of HSulf-1 and HSulf-2. This hypothesis is confirmed by staining tumors with Masson's trichrome, which stains collagen blue and reveals intense concentration of collagen within the ECM of Sulf-expressing tumors, but very little collagen in control tumors (Fig. 5B, bottom row).

**Expression of Sulf in Vivo Inhibits Assembly of the FGF-2 Signaling Complex on the Tumor Cell Surface**—To confirm that the Sulf s are enzymatically active within the *in vivo* tumor microenvironment, we investigated FGF-2 signaling. Previous studies have shown that the FGF-2 ternary signaling complex composed of FGF-2, heparan sulfate, and the FGF receptor 1c, FGF-2·HS·FR1c, can be assembled *in situ* on tissue sections utilizing the endogenous tissue heparan sulfate and exogenous FGF-2 and FR1c (25). Because incorporation of FR1c into the complex is dependent on the presence of 6-*O*-sulfate on the heparan sulfate chains, we reasoned that if the Sulf s were actively removing these sulfate groups *in vivo*, the FR1c would not be incorporated into the complex on the surface of the tumor cells. As expected, binding of FGF-2 alone was equivalent among tumors formed by either control or Sulf-transfected cells, because FGF-2 binding does not require 6-*O*-sulfation (Fig. 6, B, E, and H). This finding, along with antibody 3G10 staining (Fig. 6, A, D, and G), confirms the notion that levels of heparan sulfate on tumor cell surfaces are equivalent among the Sulf and control groups. However, in Sulf-expressing tumors, FR1c binding to the FGF-2·heparan sulfate complex at the tumor cell surface was dramatically reduced as compared with control tumor cells that bind high levels of the receptor (Fig. 6, C, F, and I). This finding confirms that the Sulf s expressed by tumors growing *in vivo* are actively removing 6-*O*-sulfate from the tumor cells. Interestingly, the effects of the sulf enzymes appear to be restricted to the tumor cell surface, because there was strong FR1c binding to the stromal areas that are high in ECM heparan sulfate. This positive staining within the ECM for FR1c in the Sulf-expressing tumors also serves as an excellent internal control.

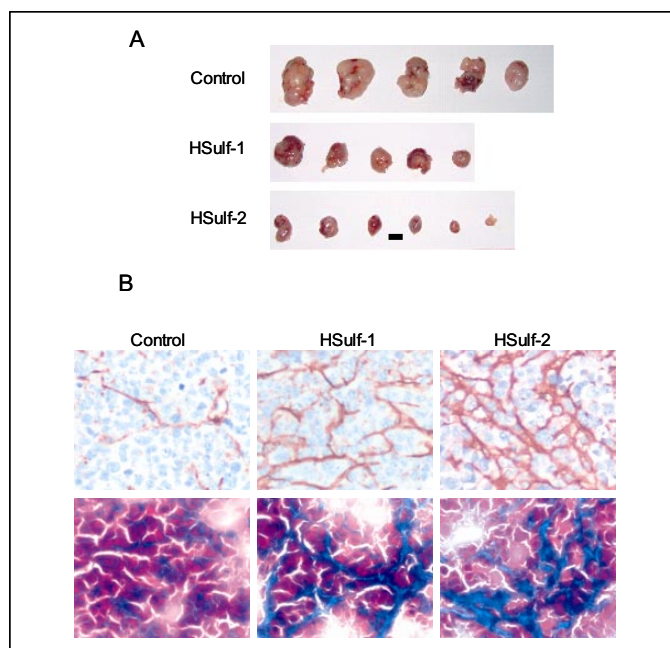


FIGURE 5. **Sulf expression inhibits tumor growth and promotes ECM deposition.** A, tumors were harvested 7 weeks after subcutaneous injection and photographed. Bar, 1 cm. B, top row, heparan sulfate present on sections of primary tumors was identified by 10E4 staining. Note the intense staining within the cords of the extracellular matrices of tumors expressing HSulf-1 or HSulf-2 as compared with controls. Very little 10E4 staining is detected on tumor cell surfaces. Bottom row, primary tumors were stained with Masson's trichrome stain, which colors collagen blue and nuclei and cytoplasm red.

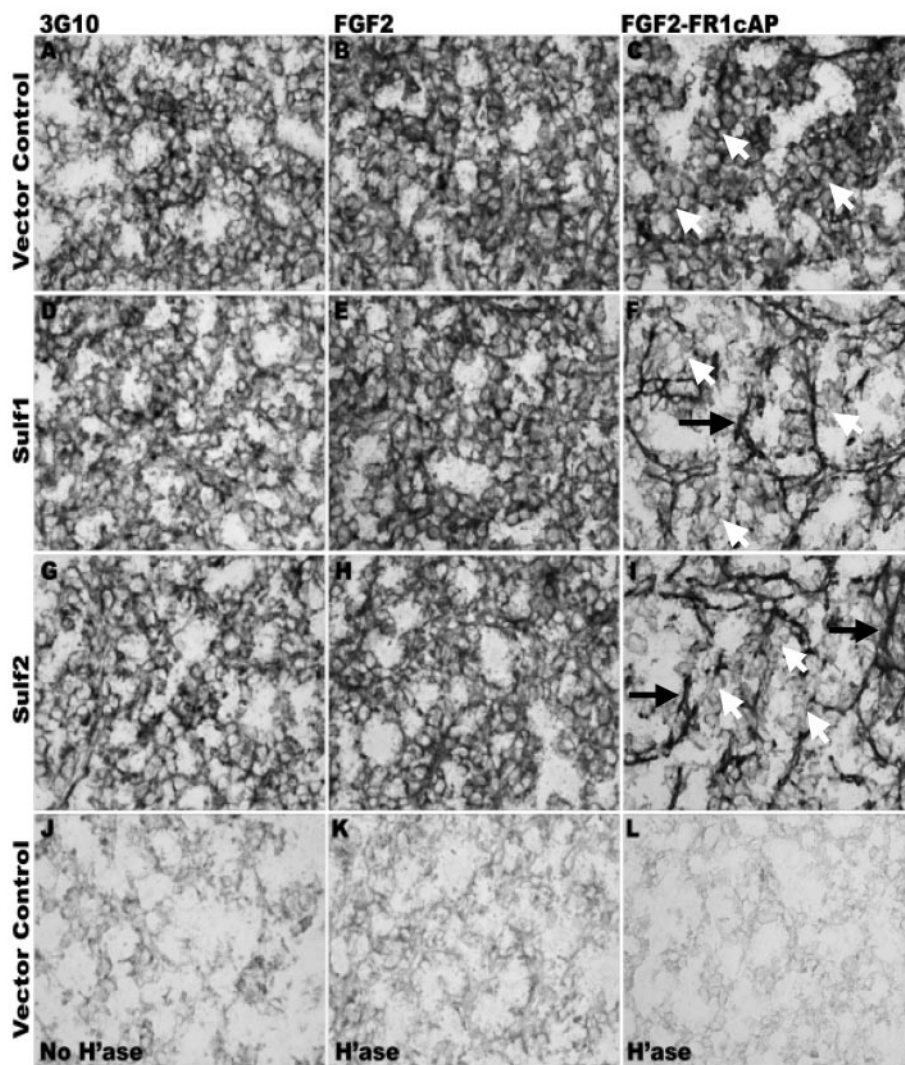
## DISCUSSION

Previous studies have implicated heparan sulfate 6-*O*-endosulfatases in the regulation of tumor cell growth control *in vitro*. We now provide strong evidence that Sulf s act to inhibit myeloma tumor growth *in vivo*. Following injection of myeloma tumor cells expressing elevated levels of Sulf s, the growth of tumors in SCID mice is dramatically suppressed as compared with controls (>5-fold suppression by HSulf-1 and 10-fold suppression by HSulf-2). Because the CAG myeloma cells used in this study represent a highly aggressive cancer phenotype (26), our results indicate that Sulf activity is a potent inhibitor of tumor growth and progression *in vivo*. Thus modulation of Sulf activity within the tumor microenvironment may be a critical determinant of malignant behavior. In addition, we made the following findings. (i) HSulf-2 and HSulf-1 have very similar biological effects on tumor cell behavior. (ii) The extracellular activity of Sulf s *in vivo* is restricted to the tumor cell surface. (iii) The Sulf s promote enhanced deposition of ECM within the tumor stroma.

To date, endosulfatases that specifically remove 6-*O*-sulfation have been described in quail, rat, mouse, and human (5, 7, 8). As reported previously for HSulf-1 and HSulf-2 expressed in Chinese hamster ovary cells (7), we found detectable levels of the enzymes in conditioned media of transfected myeloma cells (Fig. 1), supporting the notion that these enzymes act within the extracellular environment to modify heparan sulfate chains on the surface of cells. This hypothesis was confirmed by disaccharide analysis of cell surface heparan sulfate showing that levels of 6-*O*-sulfate groups of trisulfated disaccharides were substantially diminished as compared with controls (TABLE ONE).

Although others have demonstrated that HSulf-1 can regulate growth factor signaling and tumor cell growth *in vitro*, there have been no reports on the effect of HSulf-2 on cell behavior. We find that, in general, the effects of HSulf-2 parallel those of HSulf-1 both *in vitro* and *in vivo*. This includes attenuation of FGF-2 signaling as well as growth

**FIGURE 6. Expression of Sulf inhibits assembly of the FGF-2 ternary signaling complex on tumor cells growing *in vivo*.** A, D, and G, the distribution of heparan sulfate on tumors formed from control, HSulf-1-transfected, and HSulf-2-transfected cells is similar as determined by staining with mAb 3G10 after heparitinase treatment of the tumor sections. Sections without heparitinase treatment were used as the control, and the image from one sample is shown (J). B, E, and H, binding of FGF-2 to tumor sections is also similar among the three groups and coincided with the heparan sulfate distributions as revealed by monoclonal antibody 3G10 staining. FGF-2 binding was greatly reduced on sections pretreated with heparin lyases (K), indicating that binding of FGF-2 to the tissue sections is mediated by heparan sulfate. C, F, and I, on tumors formed by cells transfected with either HSulf-1 or HSulf-2, the FGF-2·HS-FR1c complex is not extensively assembled at the tumor cell surface (white arrows). In contrast, surfaces of tumor cells in control tumors exhibit high levels of complex formation (white arrows). Note that extensive FGF-2·HS-FR1c complex formation does occur within the ECM of the tumors expressing Sulfs (F and I, black arrows), indicating that the heparan sulfate present in this location is not 6-O-desulfated. FGF-2·FR1c complex formation is heparan sulfate-dependent, because prior treatment of tissue sections with heparitinase abolishes binding (L).



inhibition. However, at least in the present study, HSulf-2 overall was a more potent inhibitor of tumor growth than HSulf-1 (Figs. 4 and 5A).

Interestingly, our data indicate that the range of activity of the endosulfatases may be limited *in vivo*. This notion is suggested by the finding that the ternary signaling complex for FGF-2 was assembled within the tumor stroma but not on the surface of tumor cells (Fig. 6). This implies that heparan sulfates on the tumor cells are altered but that heparan sulfate within the stromal ECM remains 6-O-sulfated. That the stromal heparan sulfate is normal is further supported by our finding that microvessel density of the tumors formed in the presence of Sulfs is similar to that in control tumors not expressing enhanced levels of the enzymes (data not shown). A restricted local effect of Sulfs is consistent with those reported previously showing that QSulf-1 expression alters only the heparan sulfate on the cell expressing the enzyme, not the heparan sulfate on adjacent cells that lack QSulf-1 expression (4). It is also consistent with the notion that Sulfs can act to regulate growth factor tissue gradients during development (3). Together, these results indicate that the growth suppressing effects of the Sulfs in myeloma tumors are related to their remodeling of heparan sulfate on the tumor cell surface rather than the heparan sulfate in the ECM, which is not altered by Sulfs.

Although Sulf expression does not have a direct effect on 6-O-sulfation within the tumor ECM, it does enhance ECM deposition within

tumors. This finding was first made evident by comparing levels of antibody 10E4-positive heparan sulfate between controls and Sulf-expressing tumors (Fig. 5). More heparan sulfate staining is present in the sulf-expressing tumors than in the controls, and staining is predominantly in the tumor stroma. This was also reflected by the elevated level of FR1c binding to heparan sulfate in the ECM of Sulf-expressing tumors, and by Masson's trichrome stain, which shows that there are more collagen fibrils present in the Sulfs than in the controls (Figs. 5C and 6, C, F, and I). This is the first report showing that Sulf expression can lead to enhanced deposition of ECM in tumors. That effect could be due to increased production or assembly of ECM or to an alteration in the rate of degradation of ECM macromolecules. ECM is known to regulate gene expression and angiogenesis, and an increase in collagen content enhances mechanical stiffness, thereby inhibiting growth of tumors (27, 28). Because ECM binds to and regulates the activity of growth factors, the enhanced level of matrix molecules may shift the balance of available factors in favor of slower growth. Thus, the increase in ECM deposition could have a direct impact on tumor growth, leading to the growth inhibitory effect of the Sulfs that we observed. Similar to what we find with the Sulfs, expression of the SPARC/osteonectin protein promotes enhanced ECM deposition, leading to diminished tumor growth in mice (29, 30). It will be important to determine the mecha-

## Extracellular Sulfatase Inhibits Tumor Growth *in Vivo*

nism by which the Sulfs enhance ECM deposition and, specifically, how this impacts tumor behavior.

In previous studies on several cell types, a reduction in 6-*O*-sulfation led to a loss of antibody 10E4 reactivity with heparan sulfate (4, 9, 11). Contrary to this finding, in the myeloma cells studied here a reduction in 6-*O*-sulfation had no effect on 10E4 staining (Fig. 1). The 10E4 epitope is not clearly defined, although previous work has shown that *N*-sulfation of heparan sulfate is required for 10E4 reactivity (16). Whether 6-*O*-sulfation is part of the epitope remains to be determined, but our results suggest that 10E4 binds strongly to heparan sulfate even when sulfation levels at the 6-*O*-position are low. Perhaps because 10E4 is an IgM and, thus, pentameric, epitope recognition is highly dependent on the organization of heparan sulfate on the cell surface. Effective assembly of a recognizable epitope may require clustering of heparan sulfate. Removal of 6-*O*-sulfation may alter heparan sulfate organization on some cells in such a way that the 10E4 epitope is lost, whereas on other cells, such as the myeloma cells studied here, there is no effect on the 10E4 epitope. Another interesting observation related to 10E4 is the low level of staining observed on the surface of both control and Sulf-transfected tumor cells growing *in vivo* (Fig. 4). Because 3G10 staining of tumor tissues demonstrates that heparan sulfate is abundant on these tumor cells (Fig. 6), it is suggested that the 10E4 epitope is masked *in vivo*. This possibility is supported by the observation that 10E4 staining is present on cells growing *in vitro* (Fig. 1) but then lost on tumors growing *in vivo*. Also, it was noted previously that tissue staining patterns of 3G10 and 10E4 are not superimposable, probably because of differences in epitope accessibility or heparan sulfate structure (16).

Although we do not know if attenuation of FGF signaling is responsible for the growth inhibitory effects seen in our *in vivo* experiments, we used the FGF-2 signaling pathway to verify that sulfatase was exerting biological effects both *in vitro* and *in vivo*. *In vitro* we found that expression of either Sulfs results in reduced phosphorylation of ERK-1 and ERK-2 (Fig. 2). This is similar to results on various cancer cell lines, demonstrating that HSulf-1 can inhibit signaling of several heparin binding growth factors including FGF-2, HGF, and heparin binding epidermal growth factor (9–12). We also confirmed *in vivo* that the Sulfs were enzymatically active by demonstrating a loss in the ability of tumor cells to assemble the ternary FGF-2·HS·FR1c complex (Fig. 6). The loss of signaling via heparin-binding growth factors could inhibit myeloma tumor growth. For example, HGF is overexpressed by tumor cells in many myeloma patients and thus may be critical in driving the disease (26). Moreover, *in vitro* studies indicate that HGF activity in myeloma cells is dependent on the heparan sulfate chains of syndecan-1 (31). Thus, modulation of heparan sulfate chains by Sulfs could have a dramatic impact in myeloma by attenuating growth signals promoted by HGF. Studies are now underway to examine the effects of Sulfs on the growth of HGF-dependent myeloma cell lines.

Although the role of Sulfs in cancer is still poorly understood, our results provide the first direct evidence that these enzymes can suppress tumor growth *in vivo*. This is consistent with *in vitro* studies of cell lines and with studies on tumor tissues revealing that HSulf-1 is often down-regulated in cancer (9). However, it cannot be assumed that expression of Sulfs is always a negative regulator of tumor growth, because in some tumor tissues the levels of expression are high, whereas in other tumors the expression is low (9–12). One critical factor determining the effect of Sulfs in cancer is the growth factors that may be driving a specific tumor. For example, cancers driven by Wnt signaling would likely be enhanced by Sulf activity, whereas those driven by FGF-2 or HGF would be inhibited by Sulfs. Another critical determinant may be the activity state of the enzyme and how its activity is regulated. Additionally, Sulf

expression may be lost as tumors become more aggressive, either because of changes in the tumor cells themselves or because of the tumor microenvironment. In this context it is important to note that the effect of Sulf expression seems to be related to the tumor microenvironment, because the growth of cells *in vitro* is not inhibited by Sulfs, whereas growth *in vivo* is significantly inhibited.

The mechanisms responsible for misregulation of *sulf* genes in cancer are not understood. HSulf-1 is located at chromosome 8q13.2 near the *c-myc* gene, leading to speculation that HSulf-1 up-regulation results from its co-amplification with *c-myc* in some cancers (11). Studies of hepatocellular carcinomas demonstrate that in these cells diminished HSulf-1 expression may be due to loss of heterozygosity or from hypermethylation of HSulf-1 regulatory sequences (11). Treatment of these carcinomas with the DNA methylase inhibitor 5-aza-2'-deoxycytidine restores HSulf-1 expression. There is currently no information available on the regulation of HSulf-2, although Affymetrix gene array analysis of myeloma tumor cells revealed that HSulf-2 was highly overexpressed in a subset of patients, whereas HSulf-1 levels remained low.<sup>3</sup> The significance of this finding remains to be determined, but because Sulfs promote Wnt signaling the elevated HSulf-2 could be in response to signals from the myeloma bone microenvironment where the Wnt signaling pathway is often misregulated (32).

Enzymatic remodeling of heparan sulfate proteoglycan structure and function within the tumor microenvironment is emerging as an important mechanism for dynamic regulation of tumor growth (33). In addition to the inhibitory role of Sulfs described here, two other forms of enzymatic remodeling are known to occur in myeloma and other tumors. These include proteoglycan shedding from the cell surface, which promotes myeloma growth and metastasis *in vivo*, and fragmentation of heparan sulfate chains by heparanase, which promotes tumor growth, angiogenesis, and metastasis in a number of cancers (17, 34). These three known enzymatic mechanisms (sulfatases, sheddases, and heparanase), which are active within the tumor microenvironment, point out the importance of regulated remodeling of heparan sulfate proteoglycans. Moreover, the designing of novel agents that regulate these remodeling processes represents a new opportunity for therapeutic control of malignant cell growth.

*Acknowledgments*—We thank Dr. Steven D. Rosen (University of California, San Francisco) for vectors containing the HSulf-1 and HSulf-2 cDNA, Dr. Charles P. Emerson, Jr. (Boston Biomedical Institute) for polyclonal antibodies against Sulfs, and Drs. Fenghuang Zhan and John Shaughnessy, Jr. (University of Arkansas for Medical Sciences) for sharing unpublished data on expression of HSulf-2 in myeloma patients. We also thank Dr. Guido David (University of Leuven) for helpful discussions regarding the 10E4 epitope.

## REFERENCES

1. Selva, E. M., and Perrimon, N. (2001) *Adv. Cancer Res.* **83**, 67–80
2. Esko, J. D., and Selleck, S. B. (2002) *Annu. Rev. Biochem.* **71**, 435–471
3. Viviano, B. L., Paine-Saunders, S., Gasiunas, N., Gallagher, J., and Saunders, S. (2004) *J. Biol. Chem.* **279**, 5604–5611
4. Ai, X., Do, A. T., Lozynska, O., Kusche-Gullberg, M., Lindahl, U., and Emerson, C. P., Jr. (2003) *J. Cell Biol.* **162**, 341–351
5. Dhoot, G. K., Gustafsson, M. K., Ai, X., Sun, W., Standiford, D. M., and Emerson, C. P., Jr. (2001) *Science* **293**, 1663–1666
6. Wang, S., Ai, X., Freeman, S. D., Pownall, M. E., Lu, Q., Kessler, D. S., and Emerson, C. P., Jr. (2004) *Proc. Natl. Acad. Sci. U. S. A.* **101**, 4833–4838
7. Morimoto-Tomita, M., Uchimura, K., Werb, Z., Hemmerich, S., and Rosen, S. D. (2002) *J. Biol. Chem.* **277**, 49175–49185
8. Ohto, T., Uchida, H., Yamazaki, H., Keino-Masu, K., Matsui, A., and Masu, M. (2002) *Genes Cells* **7**, 173–185

<sup>3</sup> F. Zhan and J. D. Shaughnessy, Jr., unpublished observations.

9. Lai, J., Chien, J., Staub, J., Avula, R., Greene, E. L., Matthews, T. A., Smith, D. I., Kaufmann, S. H., Roberts, L. R., and Shridhar, V. (2003) *J. Biol. Chem.* **278**, 23107–23117
10. Lai, J. P., Chien, J., Strome, S. E., Staub, J., Montoya, D. P., Greene, E. L., Smith, D. I., Roberts, L. R., and Shridhar, V. (2004) *Oncogene* **23**, 1439–1447
11. Lai, J. P., Chien, J. R., Moser, D. R., Staub, J. K., Aderca, I., Montoya, D. P., Matthews, T. A., Nagorney, D. M., Cunningham, J. M., Smith, D. I., Greene, E. L., Shridhar, V., and Roberts, L. R. (2004) *Gastroenterology* **126**, 231–248
12. Li, J., Kleeff, J., Abiatari, I., Kayed, H., Giese, N. A., Felix, K., Giese, T., Buchler, M. W., and Friess, H. (2005) *Mol. Cancer* <http://www.molecular-cancer.com/content/4/1/14>
13. Borset, M., Hjertner, O., Yaccoby, S., Epstein, J., and Sanderson, R. D. (2000) *Blood* **96**, 2528–2536
14. Yang, Y., Macleod, V., Bendre, M., Huang, Y., Theus, A. M., Miao, H. Q., Kussie, P., Yaccoby, S., Epstein, J., Suva, L. J., Kelly, T., and Sanderson, R. D. (2005) *Blood* **105**, 1303–1309
15. Rhomberg, A. J., Ernst, S., Sasisekharan, R., and Biemann, K. (1998) *Proc. Natl. Acad. Sci. U. S. A.* **95**, 4176–4181
16. David, G., Bai, X. M., Van der Schueren, B., Cassiman, J.-J., and Van den Berghe, H. (1992) *J. Cell Biol.* **119**, 961–975
17. Yang, Y., Yaccoby, S., Liu, W., Langford, J. K., Pumphrey, C. Y., Theus, A., Epstein, J., and Sanderson, R. D. (2002) *Blood* **100**, 610–617
18. Ornitz, D. M., Yayon, A., Flanagan, J. G., Svahn, C. M., Levi, E., and Leder, P. (1992) *Mol. Cell Biol.* **12**, 240–247
19. Allen, B. L., Filla, M. S., and Rapraeger, A. C. (2001) *J. Cell Biol.* **155**, 845–858
20. Flanagan, J. G., Cheng, H. J., Feldheim, D. A., Hattori, M., Lu, Q., and Vanderhaeghen, P. (2000) *Methods Enzymol.* **327**, 19–35
21. Flanagan, J. G., and Leder, P. (1990) *Cell* **63**, 185–194
22. Pye, D. A., Vives, R. R., Turnbull, J. E., Hyde, P., and Gallagher, J. T. (1998) *J. Biol. Chem.* **273**, 22936–22942
23. Rusnati, M., Coltrini, D., Caccia, P., Dell'Era, P., Zoppetti, G., Oreste, P., Valsasina, B., and Presta, M. (1994) *Biochem. Biophys. Res. Commun.* **203**, 450–458
24. Guimond, S., Maccarana, M., Olwin, B. B., Lindahl, U., and Rapraeger, A. C. (1993) *J. Biol. Chem.* **268**, 23906–23914
25. Chang, Z., Meyer, K., Rapraeger, A. C., and Friedl, A. (2000) *FASEB J.* **14**, 137–144
26. Zhan, F., Hardin, J., Kordsmeier, B., Bumm, K., Zheng, M., Tian, E., Sanderson, R., Yang, Y., Wilson, C., Zangari, M., Anaissie, E., Morris, C., Muwalla, F., van Rhee, F., Fassas, A., Crowley, J., Tricot, G., Barlogie, B., and Shaughnessy, J., Jr. (2002) *Blood* **99**, 1745–1757
27. Monsky, W. L., Mouta Carreira, C., Tsuzuki, Y., Gohongi, T., Fukumura, D., and Jain, R. K. (2002) *Clin. Cancer Res.* **8**, 1008–1013
28. Netti, P. A., Berk, D. A., Swartz, M. A., Grodzinsky, A. J., and Jain, R. K. (2000) *Cancer Res.* **60**, 2497–2503
29. Puolakkainen, P. A., Brekken, R. A., Muneer, S., and Sage, E. H. (2004) *Mol. Cancer Res.* **2**, 215–224
30. Brekken, R. A., Puolakkainen, P., Graves, D. C., Workman, G., Lubkin, S. R., and Sage, E. H. (2003) *J. Clin. Investig.* **111**, 487–495
31. Derksen, P. W., Keehnen, R. M., Evers, L. M., van Oers, M. H., Spaargaren, M., and Pals, S. T. (2002) *Blood* **99**, 1405–1410
32. Tian, E., Zhan, F., Walker, R., Rasmussen, E., Ma, Y., Barlogie, B., and Shaughnessy, J. D., Jr. (2003) *N. Engl. J. Med.* **349**, 2483–2494
33. Sanderson, R. D., Yang, Y., Kelly, T., MacLeod, V., Dai, Y., and Theus, A. (2005) *J. Cell Biochem.*, in press
34. Vlodavsky, I., Goldshmidt, O., Zcharia, E., Atzmon, R., Rangini-Guatta, Z., Elkin, M., Peretz, T., and Friedmann, Y. (2002) *Semin. Cancer Biol.* **12**, 121–129